Published in final edited form as:
J Phys Conf Ser. 2013 ; 425: . doi:10.1088/1742-6596/425/1/012006.

Predicted optical performance of the GM/CA@APS micro-focus beamline

Robert F. Fischetti[a], **Derek Yoder**[a], **Shenglan Xu**[a], **Oleg Makarov**[a], **Craig Ogata**[a], and **Janet L. Smith**[b]

Robert F. Fischetti: rfischetti@anl.gov

[a]GM/CA@APS, X-Ray Science Division, Advanced Photon Source, Argonne National Laboratory, Argonne, IL 60439, USA

[b]Life Sciences Institute, Department of Biological Chemistry, University of Michigan, Ann Arbor, MI 48109, USA

Abstract

GM/CA at the APS has developed microcrystallography capabilities for structural biology applications. The robust, quad, mini-beam collimators, which enable users to rapidly select between a 5, 10 or 20 micron diameter beam or a scatter guard for the full focused beam, are coupled with several powerful automated software tools that are built into the beamline control system JBluIce-EPICS. Recent successes at beamlines around the world in solving structures from microcrystals (2 – 10 microns) have led to increased demand for high-intensity micro-focus beams. We have designed a new micro-focus endstation to increase the intensity in mini- and micro-beams at GM/CA by one to two orders of magnitude to meet this growing demand. The new optical design is based on the well-established approach of using two-stage demagnification. The existing bimorph mirrors, arranged in a Kirkpatrick-Baez geometry, focus the beam onto slits located upstream of the sample whereby the slit aperture defines a secondary source, that is reimaged with a second pair of mirrors. This design incorporates two focal modes: a mini-beam mode where the beam is focused to 20-micron diameter and a micro-beam mode where it is focused to 5-microns. The size of the secondary source aperture can be varied rapidly (seconds) to adjust the beam size at the sample position in two ranges 20 – 3 micron and 5 – 1 micron. The second set of mirrors will each have two super polished ellipses allowing quick (minutes) interchange between modes.

1. Introduction

The application of microcrystallographic techniques for structure determination of biological macromolecules originated with the pioneering experiments at ID13 of the ESRF [1]. At the National Institute of General Medical Sciences and National Cancer Institute Structural Biology Facility at the Advanced Photon Source (GM/CA@APS), we developed the quad-mini-beam collimator that allowed users to rapidly select a 5, 10, or 20 μm diameter beam or a larger variable beam size with a scatter guard aperture [2,3]. We also developed the JBluIce-EPICS GUI and software tools that allow users to fully exploit the rapid beam size change [4,5]. These tools have been applied to challenging projects and resulted in the determination of several high impact structures [for example, 6,7,8,9]. Recently, we

demonstrated a reduction of radiation damage with micro-beams when energetic photoelectrons deposit a significant fraction of their energy outside the footprint of a 15-18 keV X-ray beam [10]. However, methodologies to fully exploit this effect remain to be developed, and access to a high energy (>25 keV) micro-beam will facility this potentially important new approach. In the past several years beamlines around the world have begun offering or are planning to offer microcrystallography capabilities [11]. To meet the growing demand for a highly brilliant beam with a size in the range of 1 -20 microns GM/CA is developing a new micro-focus endstation.

2. Endstation specifications

A large part of the success of the mini-beams at GM/CA is the ability for users to rapidly change the beam size. The specifications for the new endstation include extending the range over which users can rapidly change the beam size. To achieve this goal, the new specifications include both mini-beam and micro-beam modes covering the range from 1-20 μm, and the capability for rapid (seconds) change of the beam size within a mode and fast (<10 minutes) change between modes. The optical specifications for the micro-focus endstation are summarized in Table 1.

3. Optical layout

One could use a variety of different refractive or reflective optics to achieve a 1-μm beam size. However, to meet our specifications for rapid beam size change over a wide energy range, we concluded that reflective optics and two-stage demagnification was the best approach [12,13].

X-ray mirror technology has generally improved slowly over the past thirty years. The advent of adaptive optics such as “bimorph mirrors” [14] in the early 2000s significantly reduced the achievable slope error. Recently the development of “super polishing” techniques such as Elastic Emission Machining (EEM) from Osaka University [15] (commercialized by JTEC Corp.) and Ion Beam Profiling (IBP) developed at the ESRF [16] (commercialized by SESO) have proven to be far superior to conventional chemical-mechanical polishing approaches.

The proposed layout for the new endstation is shown in Figure 1. The major components of the design are a pair of existing upstream mirrors (~66 m), two sets of slits (~70.5 m and ~73 m), a set of downstream mirrors (~74.7), and the sample goniometer (75.5 m). Both sets of mirrors are arranged in the Kirkpatrick-Baez (KB) geometry. The upstream mirrors image the source onto one pair of slits thereby creating a secondary-source whose size is defined by the slit aperture so long as the aperture is smaller than the beam size at the slit position. The downstream mirrors image the secondary-source to the sample position. Single stage demagnification is sufficient to achieve a 1-μm beam in the vertical direction; however, the secondary source improves beam stability over directly imaging the source and simplifies rapidly increasing the beam size. Two-stage demagnification in the horizontal direction is required due to the large horizontal source size.

In the micro-beam mode, the upstream, bimorph mirrors curvature is adjusted to image the source to the upstream slit position (~70.5 m). The micro-focus mirrors curvature is chosen to image this secondary source to the sample position. The horizontal and vertical slit (secondary source) positions were chosen such that when the slits accept the full focused beam, the two-stage demagnification results in a circular beam of 5-μm diameter at the sample position. The beam size at the sample can be varied rapidly (seconds) from 5 μm down to 1 μm by closing the secondary source slits.

In the mini-beam mode, the upstream mirrors curvature is adjusted to image the source to the downstream slits (~73 m), and the micro-focus mirrors curvature is selected to image the downstream secondary source to the sample position. Here the slit positions were chosen so that the two-stage demagnification results in a circular beam of 20 μm diameter. The beam size at the sample can be varied rapidly (seconds) from 20 μm down to ~3 μm by closing the secondary source slits.

Switching between the micro- and mini-beam modes requires changing the curvature of the mirrors, which takes several minutes. The upstream, bimorph mirrors curvature is adjusted by recalling previously determined individual electrode voltages. The micro-focus mirrors curvature must be changed to image the respective secondary source to the sample position. If the micro-focus mirrors are bendable (mechanically or bimorph), then this can be achieved by recalling previously determined settings. However, to maximize the flux into the 1-μm beam it may be necessary to re-optimize the shape of the micro-focus mirrors. Alternatively one could use a super-polish technique to create two elliptical surfaces side-by-side on the same face of the mirror, which would provide the proper shapes for both the micro- and mini-beam modes. The focal length of the mirror could be changed by a fast (<30 sec) lateral shift between the two ellipses.

The intensity for a given beam size was calculated over the energy range of 5-40 keV using the parameters listed in Table 2. Calculated intensities and experimental values for the current single stage focusing on beamline 23-ID-D are compared in Table 3. The intensity spectrums for various beam sizes are plotted in Figure 2. The calculations took into account several factors, most of which are energy dependent: the source size, divergence and white beam intensity onto the monochromator; the monochromator bandwidth; the mirror reflectivity, angle of incidence and slope errors; the mirror and slits acceptance apertures; the geometrical magnification; the Be-window absorption; and the Al attenuators that preferentially absorb the Si(111) lower harmonic while allowing the Si(333) harmonic to pass. The upstream mirrors provide harmonic rejection over the full energy range by selecting either the mirror coating (SiO2, Rh, Pt) or mirror angle. The plots also show the advantage of using a Si(311) monochromator for energies above 20 keV; however, there is a significant decrease in intensity for lower energies.

4. Alternative approaches to rapid beam size change

A small adjustment to the mirror angle would shift the focal position downstream of the sample thereby increasing the beam size at the sample. However, all the endstation equipment following the mirrors would require realignment to the beam. While the

realignment could be automated, it would be difficult to accomplish for a 1-μm beam and would take several minutes. In addition, changing the mirror angle without changing the curvature would introduce a geometrical aberration, and the beam would have an asymmetric profile.

Another approach to increasing the beam size would be to shift the 2nd source position without changing the micro-focus mirrors curvature. This would shift the final focal position downstream of the sample and therefore increase the size at the sample position. However, this too would introduce geometrical aberrations and an asymmetric tail. In both of the above approaches, an additional consequence of shifting the focal position is that any off-focus structure in the beam would be observable at the sample position.

5. Conclusion

The proposed design is tailored to meet the growing needs of the macromolecular crystallography community for intense mini- and micro-focused beams. The final design of micro-focusing optics most likely will depend on a combination of a bendable optic or side-by-side elliptical surfaces with either EEM or IBP polishing techniques. However, the mini-beam and micro-beam modes require significantly different super-polished ellipses, and it is unclear at present whether the differences are too great to allow two super-polished ellipses on the same surface.

Acknowledgments

GM/CA@APS is supported by the National Cancer Institute(Y1-CO-1020) and the National Institute of General Medical Sciences (Y1-GM-1104). Use of the Advanced Photon Source was supported by the US Department of Energy, Basic Energy Sciences, Office of Science under contract No. DE-AC02-06CH1135.

References

1. Nelson R, Sawaya MR, Balbirnie M, Madsen AO, Riekel C, Grothe R, Eisenberg D. Structure of the cross-beta spine of amyloid-like fibrils. Nature. 2005; 435:773–778. [PubMed: 15944695]
2. Fischetti RF, Xu S, Yoder DW, Becker M, Nagarajan V, Sanishvili R, Hilgart MC, Stepanov S, Makarov O, Smith JL. Mini-beam collimator enables micro-crystallography experiments on standard beamlines. JSR. 2009; 16:217–225.
3. Sanishvili R, Nagarajan V, Yoder D, Becker M, Xu S, Corcoran S, Akey D, Smith JL, Fischetti RF. A 7 μm mini-beam improves diffraction data from small or imperfect crystals of macromolecules. Acta Cryst D. 2008; 64:425–435. [PubMed: 18391409]
4. Stepanov S, Makarov O, Hilgart M, Pothineni S, Urakhchin A, Devarapalli S, Yoder D, Becker M, Ogata C, Sanishvili R, Nagarajan V, Smith JL, Fischetti RF. JBluIce-EPICS control system for macromolecular crystallography. Acta Cryst D. 2011; 67:176–188. [PubMed: 21358048]
5. Hilgart MC, Sanishvili R, Ogata CM, Becker M, Venugopalan N, Stepanov S, Makarov O, Smith JL, Fischetti RF. Automated sample-scanning methods for radiation damage mitigation and diffraction-based centering of macromolecular crystals. J Synchrotron Radiat. 2011; 18:717–722. [PubMed: 21862850]
6. Rasmussen SG, Choi HJ, Rosenbaum DM, Kobilka TS, Thian FS, Edwards PC, Burghammer M, Ratnala VR, Sanishvili R, Fischetti RF, Schertler GF, Weis WI, Kobilka BK. Crystal structure of the human beta2 adrenergic G-protein-coupled receptor. Nature. 2007; 450:383–387. [PubMed: 17952055]
7. Rasmussen SG, DeVree BT, Zou Y, Kruse AC, Chung KY, Kobilka TS, Thian FS, Chae PS, Pardon E, Calinski D, Mathiesen JM, Shah ST, Lyons JA, Caffrey M, Gellman SH, Steyaert J, Skiniotis G,

Weis WI, Sunahara RK, Kobilka BK. Crystal structure of the β2 adrenergic receptor-Gs protein complex. Nature. 2011; 477:549–555. [PubMed: 21772288]

8. Fleishman SJ, Whitehead TA, Ekiert DC, Dreyfus C, Corn JE, Strauch EM, Wilson IA, Baker D. Computational design of proteins targeting the conserved stem region of influenza hemagglutinin. Science. 2011; 332:816–821. [PubMed: 21566186]
9. Liu W, Chun E, Thompson AA, Chubukov P, Xu F, Katritch V, Han GW, Heitman LH, IJzerman AP, Cherezov V, Stevens RC. Structural Basis for Allosteric Regulation of GPCRs by Sodium Ions. Science. 2012; 337:232–236. [PubMed: 22798613]
10. Sanishvili R, Yoder DW, Pothineni SB, Rosenbaum G, Xu S, Vogt S, Stepanov S, Makarov O, Corcoran S, Benn R, Nagarajan V, Smith JL, Fischetti RF. Radiation Damage in Protein Crystals is Reduced with a Micron-Sized X-Ray Beam. Proc Natl Acad Sci U S A. 2011; 108:6127–6132. [PubMed: 21444772]
11. Smith JL, Fischetti RF, Yamamoto M. Micro-crystallography comes of age. Curr Op Struc Biol. 2012; 22:602–612.
12. Yoder, DW.; Sanishvili, R.; Vogt, S.; Xu, S.; Makarov, O.; Benn, R.; Corcoran, S.; Fischetti, RF. One-Micron Beams for Macromolecular Crystallography at GM/CA-CAT. AIP Conference Proceedings: Tenth International Conference on Synchrotron Radiation Instrumentation; New York: Springer; 2010. p. 419-422.
13. Liu Z, Xu S, Yoder DW, Fischetti RF. Simulation and optimization of a sub-micron beam for macromolecular crystallography using SHADOW and XOP at GM/CA CAT at the APS. Proc SPIE 8129. 2011; 81290E10.1117/12.894173
14. Signorato R, Hignette O, Jose G. Multi-segmented piezoelectric mirrors as active/adaptive optics components. J Synchrotron Rad. 1998; 5:797–800.
15. Yamauchi K, Mimura H, Inagaki K, Mori Y. Figuring with subnanometer-level accuracy by numerically controlled elastic emission machining. Rev Sci Instrum. 2002; 73:4028–4033.
16. Peverini L, Kozhevnikov IV, Rommeveaux A, Vaerenbergh PV, Claustre L, Guillet S, Massonnat J-Y, Ziegler E, Susini J. Ion beam profiling of aspherical X-ray mirrors. Nucl Instr And Meth A. 2010; 616:115–118.

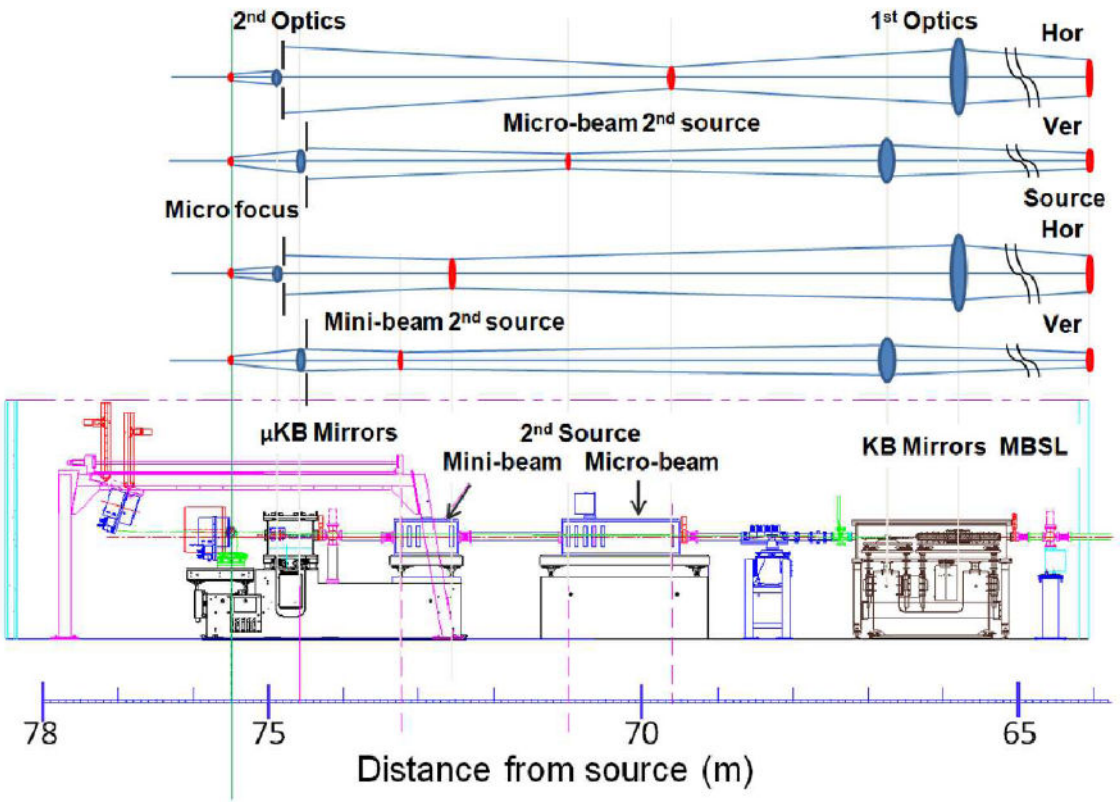

Figure 1.

The optical layout of the new endstation showing the two secondary source positions required for the mini-beam and micro-beam modes of operation. The top panel schematically illustrates the optical components, and the bottom panel depicts the elevation view of the endstation.

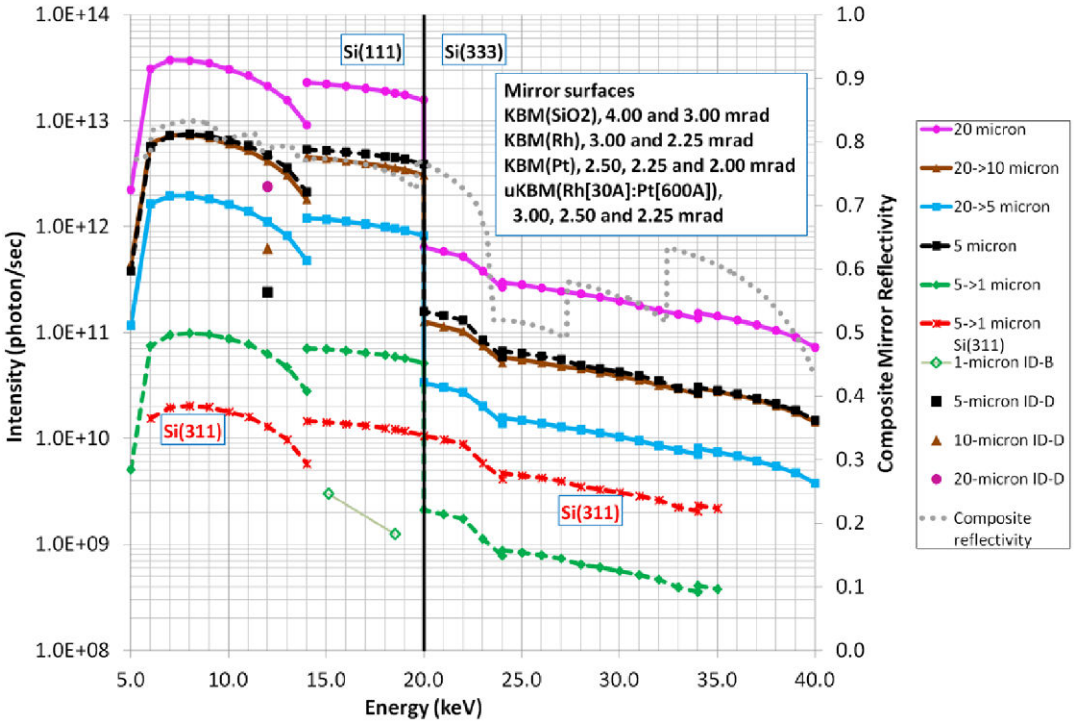

Figure 2.

The predicted intensity spectrum for various beam sizes of the micro-focus upgrade. The mini-beam family of curves derived from the 20 μm focused beam are shown with solid lines: pink (circle) 20 μm, brown (triangle) 10 μm, aqua (square) 5 μm. The micro-beam family of curves derived from the 5 μm focused beam are shown with dashed lines: black (squares) 5 μm and green (diamonds) 1 μm. The vertical line at 20 keV defines the boundary between using the monochromator fundamental reflection for Si(111), and the third harmonic Si(333). Aluminium foil of varying thickness is used to attenuate the fundamental such that the ratio of $I_{Si(333)}/I_{Si(111)} > 1000$ for all energies. The 1 μm beam with Si(311) monochromator crystals is shown with a dashed red line (stars). For reference the current mini-beam intensities are shown at 12 keV with a single symbol matching the shape and color of the same sized mini-beam curve. The two green open diamonds represent the micro-focus intensity obtained with a Fresnel zone plate for the radiation damage experiments [10]. The dotted grey curve is the product of the four mirror reflectivity curves where the angle of incidence and reflective coating of each mirror is selected to maximize the total reflectivity.

Table 1

Optical specifications for the micro-focus endstation.

Beam size	minimum ≥ 1.0 μm; maximum 20 μm (FWHM)
Energy range (keV)	6-35 using Si(111) and Si(333) or Si(311)
Harmonic rejection	$>10^4$, existing mirror system provides sufficient rejection
Micro-beam mode	1 – 5 μm with rapid (seconds) user selectable size change
Intensity in 1 μm beam	Increase at least 50-fold over current 1 μm beam*
Mini-beam mode	5 – 20 μm with rapid (seconds) user selectable size change
Mini-beam intensity	Increase at least 5-fold over current mini-beam values*
Mode switching	Quickly (<10 minutes) under user control
Positional stability:	10% RMS of focal size, 1 – 100 Hz
Intensity stability:	1% RMS noise, 1 – 100 Hz

See Table 3 for details.

Table 2

A summary of the parameters used to model the beamline performance.

	Horizontal	**Vertical**	
Source position	1.25	1.25	m
Total photon source size at 12.0 keV (FWHM)	647.4	21.5	μm
Total photon source divergence at 12.0 keV (FWHM)	29.1	13.8	μrad
Upstream (1st) mirror positions	65.80	66.75	m
Mirror length	1.05	0.60	m
Mirror slope error (RMS)	1.00	0.96	μrad
Micro-beam 2nd source	69.61	70.92	m
Mini-beam 2nd source	72.56	73.12	m
Downstream (2nd) optics	74.88	74.56	m
Mirror length	0.20	0.30	m
Mirror slope error (RMS)	0.20	0.20	μrad
Sample	75.50	75.50	m

Table 3

The calculated intensity and divergence of the new micro-focus design, the current intensity on 23-ID-D and the ratio of calculated/current intensity at 12 keV are listed. The beam size and convergence angles are reported as FWHM.

Beam size (μm) [mode]	Calculated intensity (ph/sec)	Horizontal divergence (μrad)†	Vertical divergence (μrad)†	Current intensity (ph/sec)	Intensity ratio
20 [mini]	2.1E+13	850	200	2.4E+12	8.8
10 [mini]	4.2E+12	850	200	6.2E+11	6.7
5 [mini]	1.1E+12	850	200	2.4E+11	4.6
5 [micro]	4.7E+12	850	830	2.4E+11	19.7
1 [micro]	7.5E+10	850	830	1.3E+09	60.2*

† The current divergence values on 23-ID-D are in the range 100-300 μrad.

* The intensity ratio for the 1-μm beam is for a new micro-focus setup on 23-ID-D at 12.0 keV relative to the focused beam intensity on 23-ID-B using a zone plate at 18.5 keV.